Glycerol Oxidation using MgO and Al_2O_3 supported gold and gold-palladium nanoparticles prepared in the absence of polymer stabilisers

Georgios Dodekatos[a], Laura Abis[b], Simon J. Freakley[b], Harun Tüysüz[a] and Graham J. Hutchings[b].

[a] *Max-Planck-Institut für Kohlenforschung, Kaiser-Wilhelm-Platz 1, D-45470 Mülheim an der Ruhr, Germany.*

[b] *Cardiff Catalysis Institute, Cardiff University, Main Building, Park Place, Cardiff CF103AT.*

Abstract

Au and AuPd nanoparticles supported on MgO and Al_2O_3 supports were employed for the selective aqueous phase oxidation of glycerol under basic conditions. Catalysts were prepared by sol-immobilisation without the addition of a stabilizing agent such as polyvinyl alcohol (PVA), which is generally added to stabilize the noble metal sol prior to immobilisation on. The obtained materials prepared with and without stabilizing agent were active for glycerol oxidation and showed similar catalytic performances – implying that the stabilizing polymer is not required to obtain active materials. Depending on the support used, it was possible to tailor the selectivity towards desired oxidation products by using catalysts prepared with or without stabilizing agent. PVA-free Au/γ-Al_2O_3 exhibited a remarkably high selectivity towards tartronic acid (40% at 97% conversion), which was not observed for Au/γ-Al_2O_3 prepared with PVA (27% at isoconversion). Selective glycerol oxidation performed under base-free conditions over AuPd/MgO catalysts also corroborated the previous results that the presence of a stabilizing polymer is not required to prepare active catalysts by sol-immobilisation. Thus, a facile way is presented herein to circumvent the inherent drawbacks encountered by the use of polymer stabilizers during catalyst preparation and the experimental results in fact suggest that the presence of the polymer stabilisers can affect the reaction pathways and control selectivity.

Introduction

As a by-product of biodiesel production glycerol represents a highly functionalised molecule which can itself be considered a starting material for the production of many industrially desirable products.[1-3] With the shift towards biomass derived fuels the selective functionalization of by-products from these processes will emerge as a key technology in achieving greener chemical production in the future. Selective oxidation using heterogeneous catalysis can provide a route from glycerol to valuable oxidised products such as glyceric acid, tartronic acid and dihydroxyacetone.[4-5] In these processes, the catalyst activity and selectivity is determined by factors such as the choice of metal, the control of the particle size, the nature of the support material and the pH of the reaction solution.

Monometallic Au[6-9] and bimetallic AuPd[10-12] nanoparticles have been extensively studied for the selective oxidation of glycerol under basic and base-free[13-15] conditions where high activity can be achieved with high selectivity towards C_3 oxygenates such as glyceric and tartronic acid. It has also been shown that Au/TiO_2 catalysts are capable of producing vinyl chloride monomers out of alkynes.[16] Commonly, the catalysts are prepared by a sol-immobilisation method[17] where solutions of colloidal Au and AuPd nanoparticles are formed prior to immobilisation on a high surface area support material such as TiO_2 or MgO. Usually the solutions are stabilised with polymer additives such as polyvinylpyrrolidone (PVP) or polyvinyl alcohol (PVA) to prevent coalescence of particles during the preparation. This method of preparing catalysts allows control of the nanoparticle synthesis in solution prior to immobilisation by varying the amount of polymer added and the rate of reduction using strong reductants such as $NaBH_4$.[5, 18] However, the presence of these polymers on the metal surface can lead to several disadvantages, since they can partially or completely block the access of the reactant to the metal surface, decreasing the catalyst activity, and heat treatments or refluxing treatments are typically used to remove polymers before use.[19]

Recently, the preparation of gold and gold palladium nanoparticles by colloidal methods in the absence of polymer stabilisers has been reported for both quasi-homogeneous catalysts in solution phase reduction of 4-nitrophenol[20] and supported catalysts for selective oxidation[21]. We reported that despite a larger particle size distribution, catalysts prepared without the addition of polymers were similar in activity to catalysts prepared by the extensively reported method.[21] However, the selectivity was affected by the absence of the polymer stabilisers

suggesting that the presence of polymer additives can control the reaction pathways occurring on the metal particle surface.

Here, we report the synthesis of supported monometallic and bimetallic nanoparticles of Au and AuPd by the sol-immobilisation method previously reported in the literature but without the addition of any stabiliser polymer using MgO and Al_2O_3 as support materials and reveal the extent of these effects on the catalytic performance for glycerol oxidation is highly dependent on the choice of support.

Results

We initially prepared Au colloidal solutions both in the presence and absence of a PVA stabiliser (PVA:metal = 0.65 by weight) before immobilisation on various MgO (NanoActive MgO plus (MgO_{nano}), Nanoscale Corporation, and MgO BDH (MgO_{BDH}), Analar) and Al_2O_3 (α-Al_2O_3, Aldrich, and γ-Al_2O_3, Alfa Aesar) support materials to give a nominal metal loading of 1 wt%. This method was investigated for the general applicability of preparing catalyst materials in the absence of polymers on supports other than TiO_2, since we could show that TiO_2 supported Au and AuPd NPs prepared without capping agent exhibited similar catalytic performances compared to the catalysts prepared with capping agent for benzyl alcohol and glycerol oxidation.[21] In addition, bimetallic AuPd catalysts were also prepared on MgO_{nano} with and without the addition of PVA. As depicted in

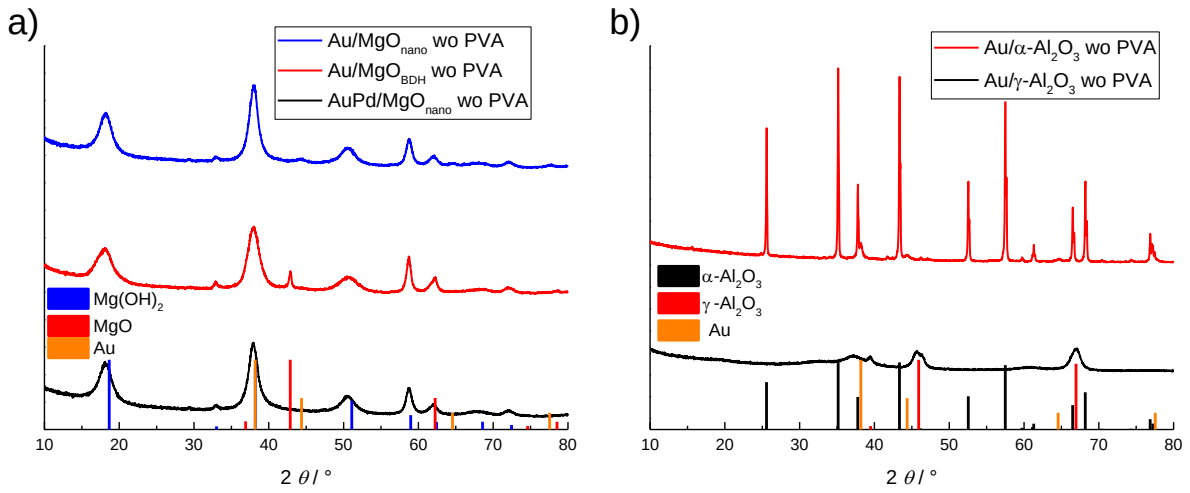

Figure 1a, Au and AuPd NP catalysts supported on MgO mainly consisted of hydrated $Mg(OH)_2$, which is due to the aqueous conditions of the sol-immobilisation procedure and is consistent with former reports.[14] The pristine supports prior to noble metal loading showed differing levels of hydration (Supporting Information, Figure S1a and b), which were

transformed to $Mg(OH)_2$ after the catalyst synthesis. No differences in the diffraction patterns of the catalyst materials can be detected between syntheses conducted with and without PVA (Supporting Information, Figure S1). Characteristic principle reflections for the Au and AuPd alloy metals cannot be observed due to the overlap with the (011) reflection of $Mg(OH)_2$ and the low amount of metal loaded. Nonetheless, a weak reflection around 45° for Au/MgO_{nano} and to a lesser extent for Au/MgO_{BDH} prepared without PVA shows that Au is deposited onto the samples. The reflection is not visible for samples prepared with PVA (Supporting Information, Figure S1 a and b) which indicates that larger Au crystallites are deposited on the surface of the surfactant-free catalysts, as it is also evidenced by TEM analysis

In the case of the Al_2O_3 supports, the γ- and α-phases can readily be identified from the diffraction patterns obtained for the catalysts prepared without PVA (Figure 1b). Both supports were loaded with Au NPs and the reflections for Au can clearly be observed for $Au/\alpha\text{-}Al_2O_3$ but remain undetected for the γ-phase. It is important to note that for the $\alpha\text{-}Al_2O_3$ the Au reflections were not observed for the sample prepared with PVA (Supporting Information, Figure S1c), which indicates a lower Au loading compared to the sample prepared without PVA and is discussed below in more detail.

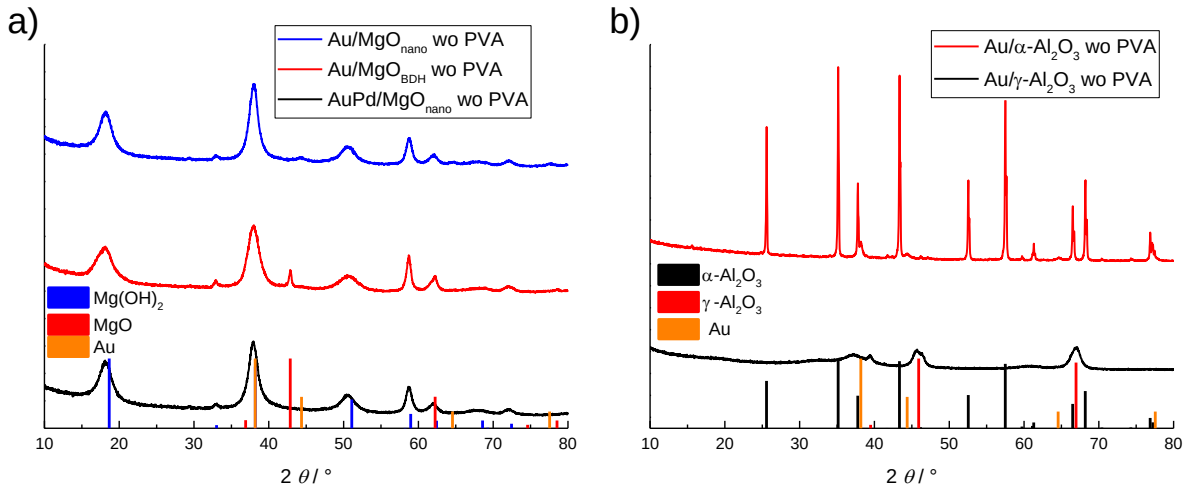

Figure 1. XRD patterns of a) Au/MgO and AuPd/MgO materials, and b) Au/Al_2O_3 materials. "wo PVA" indicates that no capping agent was used during the catalyst synthesis.

Table 1 reports the elemental analysis via MP-AES of the catalyst samples after digestion in aqua regia. The results show no significant differences in the gold loading for samples for each MgO support material prepared with PVA and without PVA suggesting that the absence of polymer does not hinder the immobilisation step significantly. The AuPd/MgO_{nano} sample prepared without PVA shows an 1:1 molar ratio determined by MP-AES for Au and Pd as expected and is comparable to the sample prepared with PVA stabilizer.

Table 1. Elemental analysis via MP-AES for Au and AuPd NPs supported on various MgO and Al_2O_3 supports prepared with (w) and without (wo) PVA during sol-immobilisation.

Sample	Nominal amount Au or Au/Pd (wt% / wt%)	Elemental analysis Au / wt% or Au/Pd (wt% / wt%)
Au/MgO_{nano} w PVA	1	0.93
Au/MgO_{nano} wo PVA	1	0.99
Au/MgO_{BDH} w PVA	1	0.81
Au/MgO_{BDH} wo PVA	1	0.80
Au/α-Al_2O_3 w PVA	1	0.1
Au/α-Al_2O_3 wo PVA	1	0.93
Au/γ-Al_2O_3 w PVA	1	1
Au/γ-Al_2O_3 wo PVA	1	0.86
AuPd/MgO_{nano} w PVA	0.65 / 0.35	0.63 / 0.33
AuPd/MgO_{nano} wo PVA	0.65 / 0.35	0.73 / 0.38

Interestingly, the deposition of Au NPs was not quantitative on α-Al_2O_3 when PVA was used as stabilizing agent (

Table 1). Only 0.1 wt% Au was determined by MP-AES instead of the expected 1 wt%. The poor immobilisation of Au on α-Al_2O_3 was also evident during the synthesis procedure. Discolouration of the Au sol after adding the support was not observed to the same extent as for the other materials, which indicates an incomplete immobilisation. Alteration of the pH during the immobilisation procedure did not improve the deposition of Au on α-Al_2O_3. On the other hand, omitting PVA under otherwise identical preparation conditions resulted in an almost complete deposition of Au. This implies that the absence of a capping agent can also be beneficial in achieving target metal deposition for the catalyst synthesis via sol-immobilisation on certain support materials. Apparently, the interaction of the naked Au NPs with the α-Al_2O_3 is stronger than the PVA-capped Au NPs. However, it is shown later that even the low-loaded PVA-capped Au/α-Al_2O_3 catalysts exhibited a remarkable high catalytic performance for glycerol oxidation. In the case of γ-Al_2O_3, no distinct differences in immobilisation were observed between stabilizer-free and PVA-capped Au NPs.

Error! Reference source not found. depicts representative XPS profiles for AuPd/MgO_{nano} catalysts between 320 and 370 eV and for Au/MgO_{nano} catalysts between 80 and 100 eV. XPS analysis of the nature of the catalyst surface is challenging due to the overlap of the Pd 3d /Au 4d region with the Mg KLL Auger structure and also the overlap of the Mg 2s region with the Au 4f photoemission peaks. Nevertheless, by comparison with similarly treated neat MgO samples, we can be confident of the Mg 2s /Au 4f fitting, which reveals solely metallic gold (binding energy between 83.2 and 83.9 eV; see Table 2) in all samples irrespective of the presence of PVA in the preparation. The shift of the Au $4f_{7/2}$ binding energies to lower values generally is an indication for ultra-small clusters (< 1 nm) or for flat, unidimensional Au particles[22], which can be excluded in our case as evidenced by TEM analysis. Another reason lies in the interaction between the Au NPs and the support which seems to be the case for the Au/MgO samples. The electron transfer from the support to the Au NP should result in the lowered $4f_{7/2}$ binding energies[22] and was previously observed for Au/MgO and Au/MgAl-LDH catalysts.[23-24] This effect is more pronounced for MgO_{BDH} than for the MgO_{nano} support (Table 2).

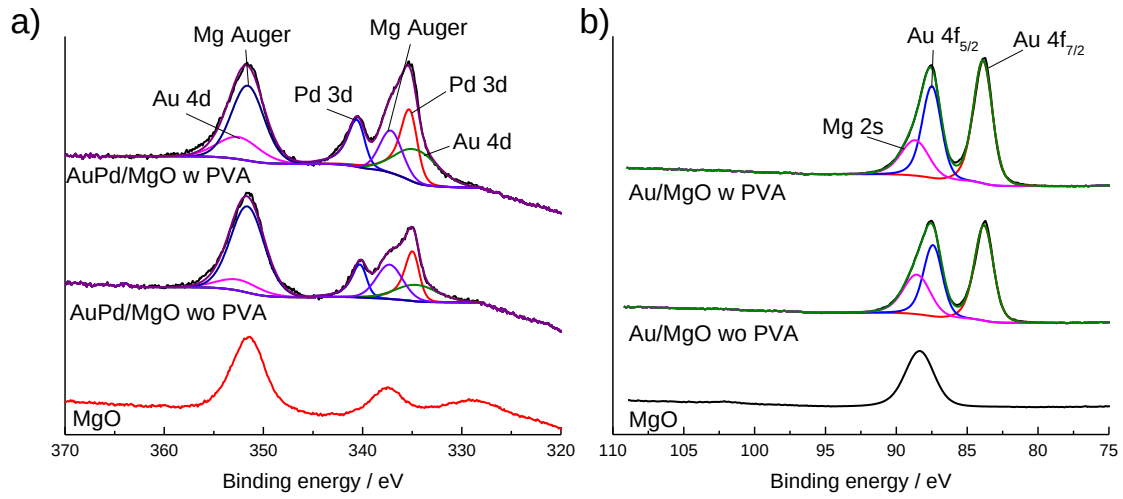

Figure 2. Representative XPS spectra of a) Au 4d and Pd 3d for AuPd/MgO_{nano}, and b) Au 4f for Au/MgO_{nano} materials prepared with (w) and without (wo) PVA during sol-immobilisation.

Due to the complications of fitting the Pd 3d region, it is not possible to accurately determine the Pd surface concentrations. However, for those where it is possible to confidently fit the Au 4d and Mg KLL Auger structure, it was determined that the Pd was in the metallic form with a BE of around 335 eV (**Error! Reference source not found.**a and Table 2).

Table 2. Physical parameters determined by TEM and XPS analysis for Au/MgO and AuPd/MgO materials prepared with and without PVA during sol-immobilisation.

Catalyst	Stabilizer	Mean Au particle size / nm	Binding energy / eV	
			Au 4f	Pd 3d
Au/MgO_{BDH}	PVA	2.6	83.2	-
	none	4.3	83.3	-
Au/MgO_{nano}	PVA	3.0	83.9	-
	none	6.5	83.8	-
$AuPd/MgO_{nano}$	PVA	7.9	83.8	335.1
	none	6.7	83.6	334.8

Transmission electron microscopy (TEM) shown in **Error! Reference source not found.** reveals that Au deposition on MgO_{nano}, MgO_{BDH}, and γ-Al_2O_3 without PVA results in bigger nanoparticles compared to the samples prepared with PVA – with, in the case of the MgO supports, a poorly shaped morphology. Samples prepared with PVA contained spherical like particles which are uniform in shape. The mean particle diameter and the particle size distributions are shown in **Error! Reference source not found.**c, f, i. Depending on the support used, the mean Au particle size is slightly changed for the PVA-capped Au NPs. Notably, γ-Al_2O_3 apparently stabilizes the PVA-free Au NPs better than the other supports.

Indeed, no deformed Au NPs are observed for these materials, which is not the case for the other supports (see Supporting Information). The MgO and α-Al_2O_3 supports (Supporting Information, Figure S2) show besides spherical Au NPs, which were taken into account for the histograms, also irregularly shaped NPs. This effect is even more pronounced for AuPd/MgO_{nano} catalysts (Supporting Information, Figure S3). The fact that the support plays a pivotal role in stabilizing the noble metal NPs has been shown previously.[17] For instance, PVA seems to be capable of stabilizing the size of Au NPs immobilized on active carbon. Tetrakis(hydroxymethyl-)phosphonium chloride (THPC) on the other hand, a weaker stabilizing agent, does not stabilize the particles on active carbon resulting in bigger Au NPs. However, by using TiO_2 as support, THPC is capable of maintaining the Au particle size after immobilisation. In fact, AuPd/TiO_2 samples prepared with and without PVA, as reported in our previous publication[20], showed only minor changes in the particle size distribution. Nonetheless, the same trend was observed that without stabilizing agent the AuPd NPs were slightly larger. Analogous samples of AuPd NPs on MgO_{nano}, however, show an inverted behaviour with respect to particle size distribution (Supporting Information, Figure S3). Samples prepared with PVA apparently have a bigger particle mean diameter compared to samples prepared without PVA. Nonetheless, the PVA seems to have a stabilizing effect on the shape of the AuPd NPs, whereas PVA-free Au NPs are highly irregular. This fact might also distort the histogram for the particle size distribution since measuring the diameter for non-spherical NPs is to some extent ambiguous.

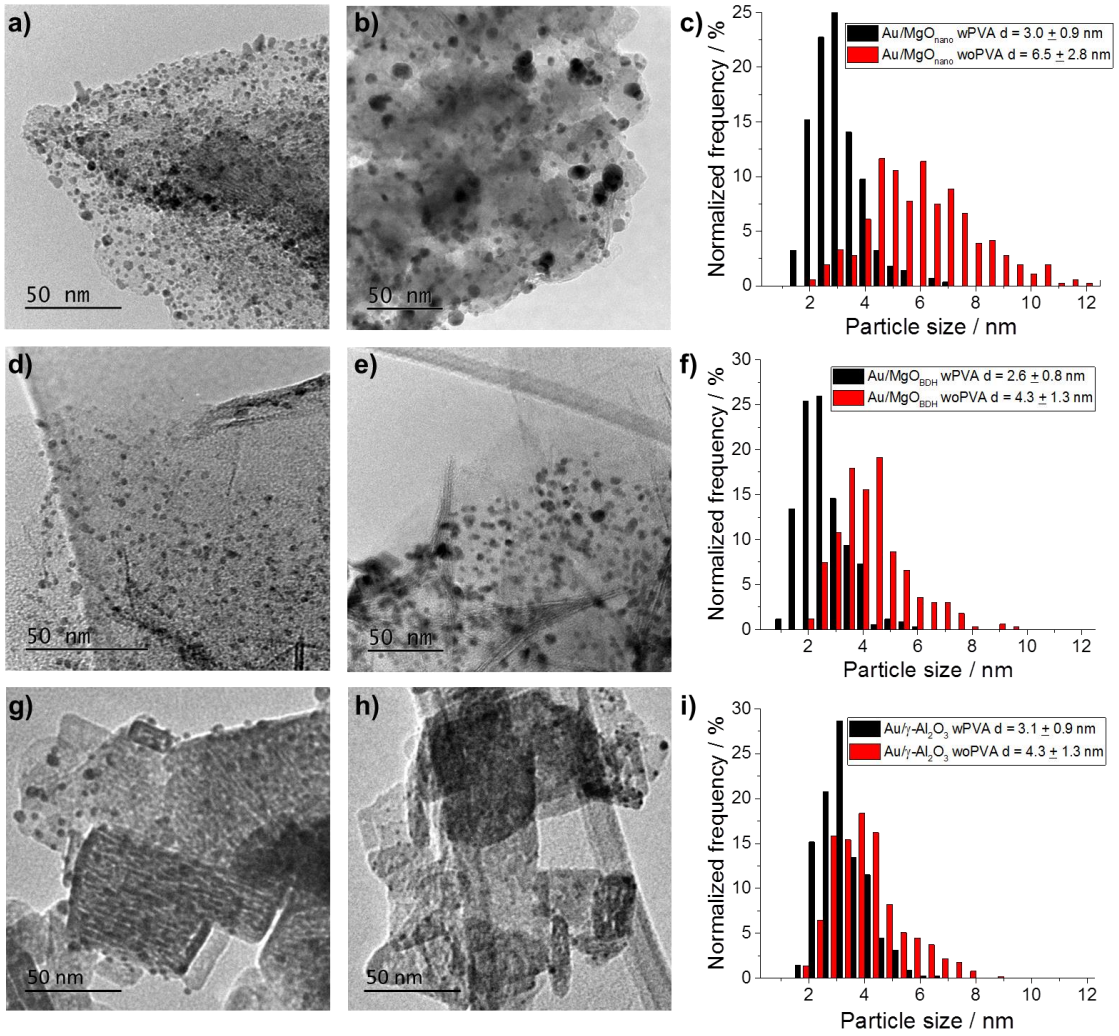

Figure 3. TEM micrographs of a), b) Au/MgO$_{nano}$, d), e) Au/MgO$_{BDH}$, and g), h) Au/γ-Al$_2$O$_3$ prepared with (w) and without (wo) PVA, respectively. c), f), i) Corresponding histograms of particle size distributions for Au NPs (at least 300 counts for each sample).

Catalytic Glycerol Oxidation

The materials prepared with and without PVA were employed for selective aqueous phase glycerol oxidation in order to investigate the effect of the polymer stabiliser on the catalytic performance. The general reaction pathway is illustrated in Scheme 1, which is based on the observations obtained in this study and of reaction pathways reported in the literature[4, 25]. The first oxidative dehydrogenation step forms glyceraldehyde or dihydroxyacetone, which are in equilibrium. Glyceraldehyde is an unstable intermediate which is readily oxidized to glyceric acid, which also can be further oxidized to form tartronic acid as consecutive product. It has to be noted that, based on the catalytic results obtained herein and reported in our previous publication,[21] tartronic acid is likely to be also a primary product formed at the catalyst

surface. Subsequently, either from glyceric acid or eventually from tartronic acid, C-C cleavage products are formed such as glycolic and oxalic acid. The formation of lactic acid follows another route over a dehydration and Cannizaro rearrangement step.

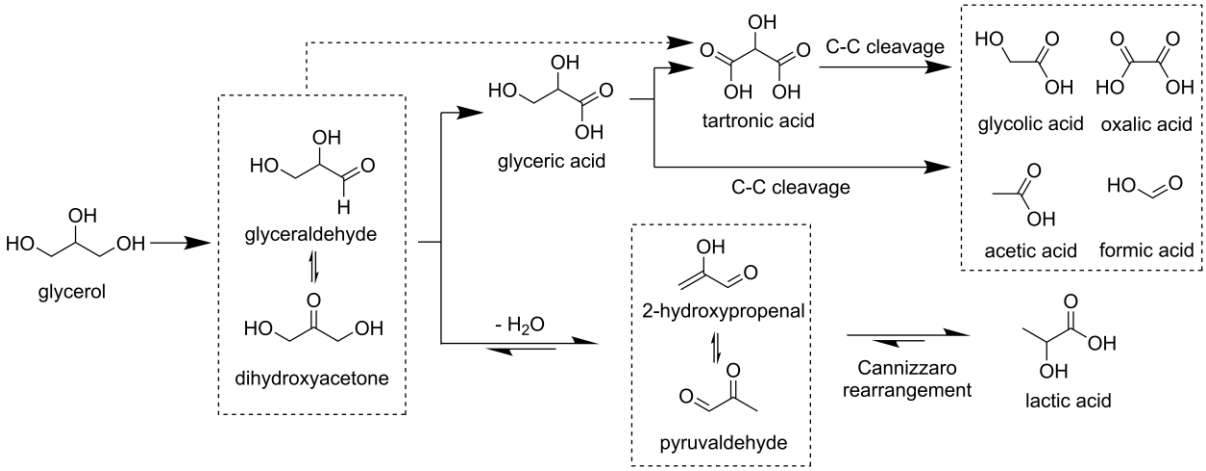

Scheme 1. General and simplified reaction scheme for glycerol oxidation according to our results and ref.[25].

As shown in Figure 4a, no significant changes in glycerol conversion can be observed between Au/MgO and Au/γ-Al_2O_3 – both catalysts reach a conversion of around 98% after 3 h reaction time. Furthermore, the effect of the capping agent used during the material synthesis on the conversion seems to be negligible. This is noteworthy since TEM characterization indicated that the preparation without capping agent resulted in larger, ill-shaped Au NPs (**Error! Reference source not found.** and Supporting Information). It is generally described in the literature that smaller Au NPs show an improved catalytic activity for glycerol oxidation.[8-9, 24-26] Hence, this observation might imply that, besides the detrimental effect on the particle morphology, the absence of PVA can have a positive impact on the catalytic performance.

Similar observations were made for Au/TiO_2 catalysts prepared with and without PVA in our previous report.[21] The activity of the catalysts reported there seems to be comparable to the activity of the monometallic catalysts presented herein, which might imply that the support does not play a pivotal role for the reaction. Nonetheless, it is shown below that by selecting the right support remarkable differences can be observed in the selectivity toward the products. Hence, the impact of the support cannot be neglected when this new synthesis approach is used in order to prepare active catalysts for glycerol oxidation.

The selectivity towards glyceric and tartronic acid is not significantly changed for Au/MgO_{BDH} catalysts (Figure 4 b). On the other hand, for Au/γ-Al_2O_3 catalysts, the impact of the capping agent on the selectivity is more obvious. The selectivity profiles depicted in

Figure 4 b) reveal that PVA-free catalysts show a higher selectivity towards tartronic acid at the expense of glyceric acid. Interestingly, PVA-free Au/γ-Al_2O_3 exhibits after 5 h reaction time a remarkably high selectivity of 42% towards tartronic acid compared to 33% for the catalysts with PVA. It has to be emphasized that the selectivities obtained for tartronic acid in this study resemble the selectivities reported by Sankar et al.[27] who achieved, as pointed out by Davis et al.[28], the highest selectivity for tartronic acid over Au/TiO_2 and Au/C catalysts but at a much higher reaction temperature of 120 °C. These catalysts were prepared by the sol-immobilisation method with PVA as stabilizing agent as presented here. Generally for monometallic catalysts, similar high selectivities were observed for Pd/C catalysts.[29] For bimetallic systems, the work of Villa et al. can be given as example where Bi-modified AuPd catalysts exhibited high selectivities towards tartronic acid.[30] In this light, it is noteworthy to mention that the absence of a stabilizing agent during the sol-immobilisation procedure can alter the catalyst properties and tailor the selectivity towards desired products in glycerol oxidation. However, it has to be pointed out that comparison of catalytic performances between papers is difficult due to the different reaction parameters, the necessity of comparing the selectivities at isoconversions, and the necessity of results free from mass transport limitations.[28]

Further supports were employed to prepare active Au/MgO and Au/α-Al_2O_3 catalysts for glycerol oxidation. As shown in Table 3, Au/MgO_{nano} catalysts prepared with and without PVA show similar conversions after 3 h reaction time (reaction profiles are presented in the Supporting Information, Figure S4 and S5). Interestingly, the presence of PVA increases the selectivity towards tartronic acid to 22% compared to 14% for the PVA-free catalyst. This trend is further enhanced after full consumption of glycerol, where it is apparent that more tartronic acid is formed at the expense of glyceric acid (Supporting Information, Figure S4). – which is in good accordance to the consecutive reaction pathway shown in Scheme 1. For Au/γ-Al_2O_3, as shown before in Figure 4 and also summarized in Table 3, the opposite is the case, where the absence of PVA during the synthesis results in a higher selectivity towards tartronic acid. In the case of Au/α-Al_2O_3, no differences in selectivities depending on the presence or absence of PVA can be observed. Hence, it can be concluded that the effect of the addition of the stabilizing agent on the catalytic performance seems to be highly dependent on the support used.

Remarkably, 0.1 wt% Au/α-Al_2O_3 catalysts prepared with PVA exhibited a similar glycerol conversion as PVA-free 1 wt% Au/α-Al_2O_3, although the Au loading for the former was highly diminished (

Table 1, for reaction profiles see Supporting Information, Figure S5). With this observation, not only could we show that a surfactant-free sol-immobilisation method allows depositing higher amounts of Au on α-Al_2O_3 (whereas with PVA this seems not possible; see above), but we also demonstrated that low Au loadings of around 0.1 wt% are sufficient for the PVA-capped Au/α-Al_2O_3 catalyst to exhibit remarkably high glycerol conversions. It is apparent that the speciation of the Au NPs plays the predominant role in the activity than the actual loaded amount, which was demonstrated also for Au/TiO_2 by Rogers et al.[31] By carefully optimizing the sol-immobilisation preparation of the catalyst, Au clusters – which were the minor species deposited on TiO_2 – contributed remarkably to the catalytic performance. A similar case might be true for 0.1 wt% Au/α-Al_2O_3 presented here, where primarily active Au species were deposited on the Al_2O_3 surface and surplus PVA-capped Au NPs were washed off. This is corroborated by the fact that PVA-capped 0.1 wt% Au/α-Al_2O_3 shows a higher mean Au particle size (7.8 nm) than PVA-free 1 wt% Au/α-Al_2O_3 (5.2 nm; Supporting Information, Figure S2). This implies that not only a decreased number of Au NPs but also a strongly decreased number of smaller Au NPs, which can still be detected by TEM analysis, is present for PVA-capped 0.1 wt% Au/α-Al_2O_3. This is in contradiction to the expectation that a high number of small Au NPs should lead to a better catalytic performance for glycerol oxidation. Hence, it might also be in this case evident that the Au speciation is the key parameter for a high activity – which, however, could not be investigated in more detail in this study. Nonetheless, the results suggest that any higher amount of Au loading contributes to the catalytic performance only to a negligible extent.

Generally, it is difficult to assign which Au particle size range of the catalysts presented is the most active for glycerol oxidation. For instance, PVA-free and PVA-capped Au/MgO and

Au/γ-Al_2O_3 exhibited different mean Au particle sizes (**Error! Reference source not found.** c, f, i) but essentially the same conversion profiles (Figure 4 and Supporting Information Figure S4) whether or not PVA was present – with changes only for the selectivities. Furthermore, no clear trend was observed for the change in selectivity with respect to the stabilizer (see above). It has to be kept in mind that superimposing effects of the stabilizer make it difficult to completely assign the catalytic results to an effect of the particle size.

Bimetallic AuPd catalysts were also deposited on MgO_{nano} and γ-Al_2O_3 to see if the preparation method with or without PVA has an influence on the catalytic performance. As shown in Figure 4c and d for AuPd/MgO_{nano} and in Table 3 for AuPd/γ-Al_2O_3 (for reaction profiles see Supporting Information Figure S6), the stabilizing agent plays no decisive role for preparing a catalyst with high activity for glycerol oxidation. Especially in the case of AuPd/MgO_{nano}, it is obvious that both catalysts, with and without PVA during the synthesis, behave essentially the same, which was also demonstrated for AuPd/TiO_2 catalysts in an earlier study conducted from some authors of the present work.[20] This is remarkable since TEM analysis (Supporting Information, Figure S3) revealed that only with the use of PVA well-formed AuPd NPs could be obtained. Also here, the particle size distribution seems to play a minor role for the catalytic performance.

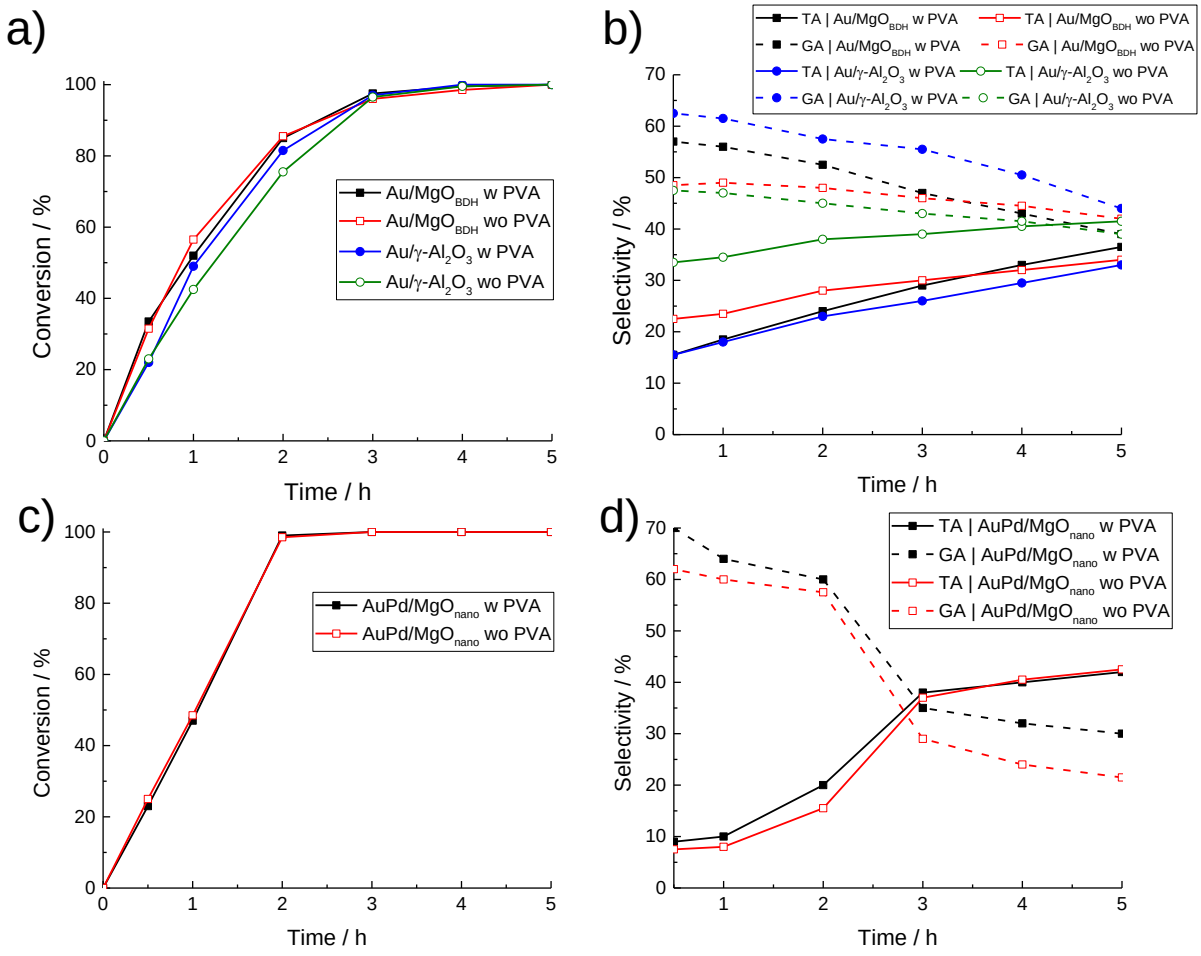

Figure 4. Conversion and selectivity profiles of glycerol oxidation for a), b) 1 wt% Au/MgO$_{BDH}$ and 1 wt% Au/γ-Al$_2$O$_3$, and c), d) AuPd (1:1 molar ratio) supported on MgO$_{nano}$. Reaction conditions: 0.3 M glycerol, 2:1 NaOH/glycerol, 500:1 glycerol/metal (for Au), 385:1 glycerol/metal (for AuPd, based on Au), 10 mL, 60 °C, 3 bar O_2, stirring speed 1200 rpm. TA: tartronic acid; GA: glyceric acid. Hollow forms denote PVA-free catalysts; solid lines indicate TA selectivity and dashed lines indicate GA selectivity.

Table 3. Summarized conversions, selectivities, and carbon mass balances for glycerol oxidation after 3 h reaction time over catalysts employed in this study. For reaction conditions see the caption in Figure 4. Generally, catalysts contained approx. 1 wt% Au loading if not otherwise specified.

Catalyst	Conversion / %	Selectivity / %							Carbon mass balance / %
		Glyceric acid	Tartronic acid	Glycolic acid	Oxalic acid	Formic acid	Lactic acid	Acetic acid	
Au/MgO$_{nano}$ w PVA	98	52	22	3	3	2	9	8	94
Au/MgO$_{nano}$ wo PVA	92	60	14	5	2	4	10	5	97
Au/MgO$_{BDH}$ w PVA	97	48	28	5	3	3	5	8	94
Au/MgO$_{BDH}$ wo PVA	95	47	29	4	4	2	4	9	92
Au/α-Al$_2$O$_3$ w PVA[a)]	76	67	7	8	1	6	9	3	98
Au/α-Al$_2$O$_3$ wo PVA	84	65	8	5	1	4	11	5	99
Au/γ-Al$_2$O$_3$ w PVA	98	55	27	4	3	3	3	6	95
Au/γ-Al$_2$O$_3$ wo PVA	97	43	40	3	6	2	1	5	98

AuPd/MgO_{nano} w PVA	100	35	38	2	9	1	10	5	89
AuPd/MgO_{nano} wo PVA	1000	32	35	2	8	2	15	6	90
AuPd/γ-Al_2O_3 w PVA	100	44	35	3	6	2	8	3	92
AuPd/γ-Al_2O_3 wo PVA	100	53	28	2	3	2	9	3	93

a) Au loading for this sample was 0.1 wt% (see

Table 1).

It is highly desired to work under base-free conditions for glycerol oxidation. In an earlier study, Hutchings and co-workers showed that MgO in conjunction with bimetallic AuPt or AuPd NPs are suitable catalysts for performing glycerol oxidation at neutral pH.[14] Hence, AuPd/MgO catalysts prepared with and without PVA were also employed for base-free glycerol oxidation and the catalytic results are presented in Figure 5. It is clearly visible that the PVA-free catalyst exhibited only a slightly inferior catalytic performance than the AuPd/MgO prepared with PVA. Moreover, the selectivity profiles show the same behaviour with only slight changes in selectivities towards glyceric acid. Also in this case it is proven that the absence of PVA during the sol-immobilisation preparation of catalysts does not show a detrimental impact on the catalytic performance for glycerol oxidation.

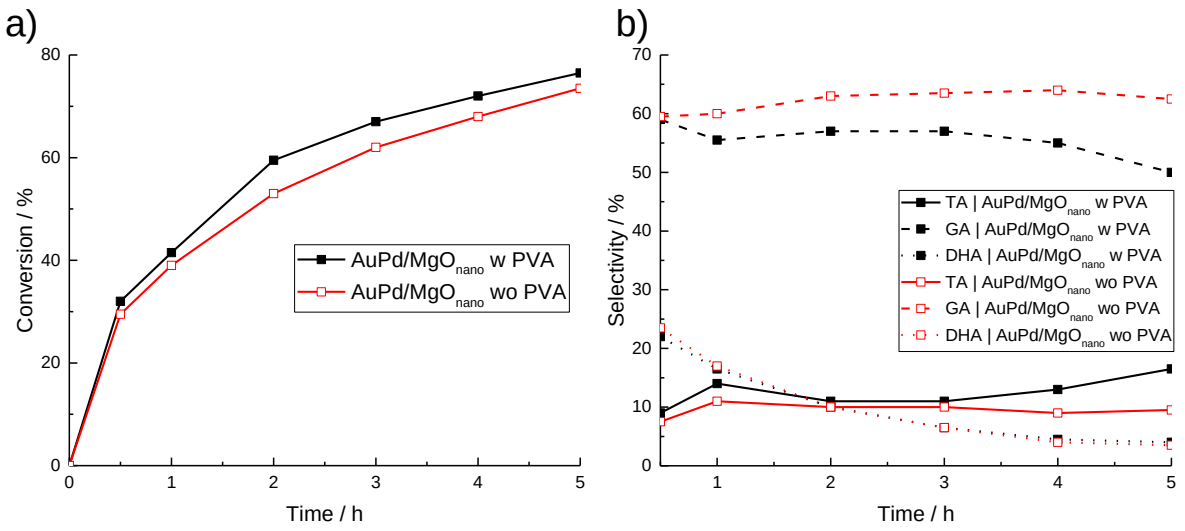

Figure 5. a) Conversion and b) selectivity profiles for glycerol oxidation under base-free conditions over 1 wt% AuPd/MgO_{nano} catalysts prepared with and without PVA during sol-immobilisation. Reaction conditions: 0.3 M glycerol, 385:1 glycerol/metal (based on Au), 10 mL, 60 °C, 3 bar O_2, stirring speed 1200 rpm. TA: tartronic acid; GA: glyceric acid; DHA: dihydroxyacetone. Hollow forms denote PVA-free catalysts; solid lines indicate TA selectivity, dashed lines indicate GA selectivity, and dotted lines indicate DHA selectivity.

Conclusions

The results presented in this study show that the absence of any stabilizing agent during the sol-immobilisation method of catalyst preparation still produces active catalysts for glycerol oxidation. In particular, it was shown that, depending on the support used, the catalytic performance either remains the same independent of the presence or absence of PVA as stabilizing agent or shows alterations in the product selectivity while maintaining similar catalytic activity. This indicates that the supports can influence the metallic Au NPs differently and, thus, result in different implications on the effect of the stabilizer on the catalytic performances. Therefore, our method allows to prepare catalysts with unprecedented catalytic properties. For instance, it was possible for Au/γ-Al_2O_3 catalysts prepared without PVA to tailor the selectivity towards tartronic acid to remarkable 40% at nearly full conversion after 3 h reaction time. On the other hand, PVA-capped or PVA-free Au/MgO, AuPd/MgO, and AuPd/γ-Al_2O_3 catalysts exhibited only negligible deviations in the catalytic performances. Up to now, mainly the effects of the type of stabilizing agent or of the used amount on the catalytic performance were investigated. It is thus remarkable that the total absence of a stabilizing agent during the sol-immobilisation synthesis still yields active catalysts for glycerol oxidation, although the Au mean particle sizes were slightly increased for the PVA-free catalysts. In addition, we demonstrated that PVA-free AuPd/MgO catalysts are also active for glycerol oxidation under base-free conditions. It is thus shown that detrimental effects by the protecting polymers, which in the past were generally inevitable for the sol-immobilisation method, can

be avoided by simply omitting their addition during the catalyst synthesis. Finally, it was shown that the sol-immobilisation technique without PVA allows a quantitative deposition of Au NPs on α-Al_2O_3, whereas with PVA only a small fraction of the Au sol was immobilized on the support; however, this small fraction revealed to be highly active for glycerol oxidation. These results pave the way for new catalyst syntheses, which might not have been possible by sol-immobilisation due to the poor noble metal sol-support interaction.

Acknowledgements

This work is supported by MAXNET Energy research consortium of the Max Planck Society and the Cluster of Excellence RESOLV (EXC 1069) funded by the Deutsche Forschungsgemeinschaft.

Experimental Section

Catalyst Preparation

$HAuCl_4 \cdot 3H_2O$ (Sigma-Aldrich, ≥49.0%), $PdCl_2$ (Sigma-Aldrich, Reagent Plus® 99%), MgO (MgO_{nano} denotes NanoActive MgO Plus from NanoScale Corporation and MgO_{BDH} denotes MgO from BDH Analar), Al_2O_3 (α-Al_2O_3, Aldrich, 99.8 %, < 10 micron; γ-Al_2O_3, Alfa Aesar, 99.97%), PVA (Sigma-Aldrich, average molecular weight MW = 9000-10000 g mol^{-1}, 80% hydrolysed), H_2SO_4 (J. T. Baker), and $NaBH_4$ (Aldrich, ≥99.99%) were used without further purification. Generally, milli-Q water (18.2 MΩ) was used for the aqueous solutions.

Monometallic Au and bimetallic AuPd NPs deposited on MgO or Al_2O_3 (in total 1 wt% metal loading) were prepared by sol-immobilisation using either PVA as stabilizing polymer ligand or without any addition of stabilizer. In a typical synthesis of 1 g of monometallic sample, an aqueous solution of $HAuCl_4 \cdot 3H_2O$ (0.8 mL, 12.5 mg mL^{-1} Au) was added to 400 mL of deionised water under vigorous stirring, followed by the addition of PVA (1 wt% aqueous solution, PVA/Au = 0.65 wt/wt). Subsequently, a freshly prepared aqueous solution of $NaBH_4$ (0.1 M, $NaBH_4$/Au = 5 mol mol^{-1},) was added rapidly into the vortex to form a red sol. After 30 min of sol generation under stirring at room temperature, the colloid was immobilised by adding 0.99 g of the desired support (MgO or Al_2O_3) and, for the Al_2O_3 supported catalyst, 8 drops of concentrated H_2SO_4. After 1 h of continuous stirring, the slurry was filtered, the catalyst washed thoroughly with deionized water (1 L) and dried at 110 °C for 16 h.

Syntheses for the bimetallic AuPd samples proceeded in the same way, but with the further addition of an aqueous $PdCl_2$ solution (6 mg mL^{-1} Pd, total metal loading 1 wt%, Au:Pd = 1 mol mol^{-1}). In this case, the stabilizer-to-metal ratio was 1.2 wt wt^{-1}. The immobilisation steps were carried out in the same manner as previously described.

For the stabilizer free variant, both monometallic and bimetallic analogues were prepared as described above but the addition of stabilizer to the preparation was omitted. The PVA-free sample was immobilised on each support after 30 min of sol generation.

Glycerol Oxidation

Glycerol oxidation under basic conditions was performed in a glass reactor (Colaver®) positioned in a thermostatically controlled oil bath at 60 °C and at 3 bar O_2 pressure, under continuous stirring (1200 rpm). Glycerol (5 mL, 0.6 M, Sigma-Aldrich, anhydrous, >99.5%) and NaOH (5 mL, 1.2 M, Sigma Aldrich BioXtra, >98%, pellets, anhydrous) were added to the reactor to give a total reaction volume of 10 mL (0.3 M glycerol, 2:1 glycerol:NaOH). The glycerol/metal mole ratio was 500:1 for the monometallic catalysts and 385:1 for the bimetallic AuPd catalysts based on Au. The total reaction time employed was 4 h, with sampling performed after 30, 60, 120 and 240 min of reaction. Samples were quenched and diluted 1:10 in deionised water before analysis by HPLC. Product analysis was carried out using an Agilent 1260 Infinity HPLC with a Metacarb 67H column with a 0.1 wt% solution of phosphoric acid as mobile phase.

Catalyst Characterization

Transmission Electron Microscopy (TEM) was performed using a JEOL 2100 microscope with a LaB_6 filament operating at 200 kV or a Hitachi H-7100 with 100 kV acceleration voltage. Samples were prepared by dispersing the powder catalyst in ethanol and allowing a drop of the suspension to evaporate on a lacey carbon film supported over a 300 mesh copper TEM grid.
XPS was performed on a Kratos Axis Ultra-DLD photoelectron spectrometer, using monochromatic Al K_α radiation at 144 W (12 mA × 12 kV) power. High resolution and survey scans were performed at pass energies of 40 and 160 eV respectively. Magnetically confined charge compensation was used to minimize sample charging and the resulting spectra were calibrated against the C 1s line at 284.7 eV. Deconvolution of the XPS spectra is complicated due to the overlap of the Au $4f_{5/2}$ peak with the Mg 2s photoelectron line. To account for this, we apply a fixed spin orbit splitting of 3.67 eV for the Au 4f doublet, with an area ratio of 4/3 and assume the FWHM of both peaks are equal.
MP-AES (Agilent 4100) was performed on the samples at the end of the reaction. The slurry was centrifuged in order to separate the solid from the liquid. The liquid was then recovered by a syringe and filtered (0.45 μm PTFE Fisherbrand®) to make sure no solid residue was left. Finally, an aliquot was appropriately diluted in order to lower the base concentration and analysed.

References

[1] M. Pagliaro, R. Ciriminna, H. Kimura, M. Rossi, C. Della Pina, *Angew. Chem. Int. Ed.* **2007**, *46*, 4434-4440.
[2] C. H. Zhou, J. N. Beltramini, Y. X. Fan, G. Q. Lu, *Chem. Soc. Rev.* **2008**, *37*, 527-549.
[3] A. Behr, J. Eilting, K. Irawadi, J. Leschinski, F. Lindner, *Green Chem.* **2008**, *10*, 13-30.
[4] B. Katryniok, H. Kimura, E. Skrzynska, J. S. Girardon, P. Fongarland, M. Capron, R. Ducoulombier, N. Mimura, S. Paul, F. Dumeignil, *Green Chem.* **2011**, *13*, 1960-1979.
[5] A. Villa, N. Dimitratos, C. E. Chan-Thaw, C. Hammond, L. Prati, G. J. Hutchings, *Acc. Chem. Res.* **2015**, *48*, 1403-1412.
[6] S. Carrettin, P. McMorn, P. Johnston, K. Griffin, G. J. Hutchings, *Chem. Commun.* **2002**, 696-697.
[7] S. Carrettin, P. McMorn, P. Johnston, K. Griffin, C. J. Kiely, G. J. Hutchings, *Phys. Chem. Chem. Phys.* **2003**, *5*, 1329-1336.

[8] S. Carrettin, P. McMorn, P. Johnston, K. Griffin, C. J. Kiely, G. A. Attard, G. J. Hutchings, *Top. Catal.* **2004**, *27*, 131-136.
[9] F. Porta, L. Prati, *J. Catal.* **2004**, *224*, 397-403.
[10] D. Wang, A. Villa, F. Porta, D. S. Su, L. Prati, *Chem. Commun.* **2006**, 1956-1958.
[11] W. C. Ketchie, M. Murayama, R. J. Davis, *J. Catal.* **2007**, *250*, 264-273.
[12] M. Sankar, N. Dimitratos, P. J. Miedziak, P. P. Wells, C. J. Kiely, G. J. Hutchings, *Chem. Soc. Rev.* **2012**, *41*, 8099-8139.
[13] A. Villa, G. M. Veith, L. Prati, *Angew. Chem. Int. Ed.* **2010**, *49*, 4499-4502.
[14] G. L. Brett, Q. He, C. Hammond, P. J. Miedziak, N. Dimitratos, M. Sankar, A. A. Herzing, M. Conte, J. A. Lopez-Sanchez, C. J. Kiely, D. W. Knight, S. H. Taylor, G. J. Hutchings, *Angew. Chem. Int. Ed.* **2011**, *50*, 10136-10139.
[15] S. A. Kondrat, P. J. Miedziak, M. Douthwaite, G. L. Brett, T. E. Davies, D. J. Morgan, J. K. Edwards, D. W. Knight, C. J. Kiely, S. H. Taylor, G. J. Hutchings, *ChemSusChem* **2014**, *7*, 1326-1334.
[16] J. Oliver-Meseguer, A. Domenech-Carbo, M. Boronat, A. Leyva-Perez, A. Corma, *Angew. Chem. Int. Ed.* **2017**, *56*, 6435-6439.
[17] S. Campisi, M. Schiavoni, C. E. Chan-Thaw, A. Villa, *Catalysts* **2016**, *6*, 21.
[18] L. Prati, A. Villa, *Acc. Chem. Res.* **2014**, *47*, 855-863.
[19] J. A. Lopez-Sanchez, N. Dimitratos, C. Hammond, G. L. Brett, L. Kesavan, S. White, P. Miedziak, R. Tiruvalam, R. L. Jenkins, A. F. Carley, D. Knight, C. J. Kiely, G. J. Hutchings, *Nat. Chem.* **2011**, *3*, 551-556.
[20] C. Deraedt, L. Salmon, S. Gatard, R. Ciganda, R. Hernandez, J. Ruiz, D. Astruc, *Chem. Commun.* **2014**, *50*, 14194-14196.
[21] L. Abis, S. J. Freakley, G. Dodekatos, D. J. Morgan, M. Sankar, N. Dimitratos, Q. He, C. J. Kiely, G. J. Hutchings, *ChemCatChem* **2017**, *9*, 2914-2918.
[22] S. Arrii, F. Morfin, A. J. Renouprez, J. L. Rousset, *J. Am. Chem. Soc.* **2004**, *126*, 1199-1205.
[23] J. Feng, C. Ma, P. J. Miedziak, J. K. Edwards, G. L. Brett, D. Li, Y. Du, D. J. Morgan, G. J. Hutchings, *Dalton Trans.* **2013**, *42*, 14498-14508.
[24] C. Xu, Z. Wang, X. Huangfu, H. Wang, *RSC Adv.* **2014**, *4*, 27337-27345.
[25] C. D. Evans, S. A. Kondrat, P. J. Smith, T. D. Manning, P. J. Miedziak, G. L. Brett, R. D. Armstrong, J. K. Bartley, S. H. Taylor, M. J. Rosseinsky, G. J. Hutchings, *Faraday Discuss.* **2016**, *188*, 427-450.
[26] N. Dimitratos, J. Lopez-Sanchez, D. Lennon, F. Porta, L. Prati, A. Villa, *Catal. Lett.* **2006**, *108*, 147-153.
[27] N. Dimitratos, A. Villa, C. L. Bianchi, L. Prati, M. Makkee, *Appl. Catal., A* **2006**, *311*, 185-192.
[28] W. C. Ketchie, Y. L. Fang, M. S. Wong, M. Murayama, R. J. Davis, *J. Catal.* **2007**, *250*, 94-101.
[29] M. Sankar, N. Dimitratos, D. W. Knight, A. F. Carley, R. Tiruvalam, C. J. Kiely, D. Thomas, G. J. Hutchings, *ChemSusChem* **2009**, *2*, 1145-1151.
[30] S. E. Davis, M. S. Ide, R. J. Davis, *Green Chem.* **2013**, *15*, 17-45.
[31] C. L. Bianchi, P. Canton, N. Dimitratos, F. Porta, L. Prati, *Catal. Today* **2005**, *102*, 203-212.
[32] A. Villa, D. Wang, G. M. Veith, L. Prati, *J. Catal.* **2012**, *292*, 73-80.
[33] S. M. Rogers, C. R. A. Catlow, C. E. Chan-Thaw, D. Gianolio, E. K. Gibson, A. L. Gould, N. Jian, A. J. Logsdail, R. E. Palmer, L. Prati, N. Dimitratos, A. Villa, P. P. Wells, *ACS Catal.* **2015**, *5*, 4377-4384.